Evidence for nonmonotonic magnetic field penetration in a type-I superconductor

V. F. Kozhevnikov,[1,2] C. V. Giuraniuc,[1,*] M. J. Van Bael,[1] K. Temst,[3] C. Van Haesendonck,[1] T. M. Mishonov,[4] T. Charlton,[5] R. M. Dalgliesh,[5] Yu. N. Khaidukov,[6] Yu. V. Nikitenko,[6] V. L. Aksenov,[6] V. N. Gladilin,[1,7,8] V. M. Fomin,[7,8] J. T. Devreese,[7] and J. O. Indekeu[9]

[1]*Laboratorium voor Vaste-Stoffysica en Magnetisme, Katholieke Universiteit Leuven, 3001 Leuven, Belgium*

[2]*Science and Mathematics Division, Tulsa Community College, Tulsa, Oklahoma 74119, USA*

[3]*Instituut voor Kern- en Stralingsfysica, Katholieke Universiteit Leuven, 3001 Leuven, Belgium*

[4]*Department of Theoretical Physics, St. Clement of Ohrid University of Sofia, 1164 Sofia, Bulgaria*

[5]*ISIS Science Division, Rutherford Appleton Laboratory, Chilton, Didcot OX11 0QX, United Kingdom*

[6]*Frank Laboratory of Neutron Physics, Joint Institute for Nuclear Research, 141980 Dubna, Moscow Region, Russia*

[7]*Theoretische Fysica van de Vaste Stoffen, Universiteit Antwerpen, 2020 Antwerpen, Belgium*

[8]*Physics of Multilayer Structures, State University of Moldova, 2009 Chisinau, Moldova*

[9]*Instituut voor Theoretische Fysica, Katholieke Universiteit Leuven, 3001 Leuven, Belgium*

(Received 2 June 2008; published 10 July 2008)

Polarized neutron reflectometry (PNR) provides evidence that *nonlocal* electrodynamics governs the magnetic field penetration in a low-κ superconductor. The sample is an In film with a large elastic mean-free path. It is shown that PNR can resolve the difference between the reflected neutron spin asymmetries predicted by the local and nonlocal theories of superconductivity. The experimental data support the nonlocal theory, which predicts a *nonmonotonic decay* of the magnetic field.

DOI: 10.1103/PhysRevB.78.012502 PACS number(s): 74.20.−z, 74.25.Ha, 78.70.Nx

In this Brief Report we pose and answer experimentally the following fundamental questions: Are nonlocal electrodynamics effects measurable in superconductors? Can the nonmonotonic decay of magnetic field penetration predicted by the nonlocal theory be observed? To what extent can polarized neutron reflectometry (PNR) resolve the difference between local and nonlocal diamagnetic responses expected for type-I superconductors?

Nonlocality is a key concept of superconductivity theory, but its experimental verification is still not established. In the Meissner state, a magnetic field applied parallel to the surface located at $z=0$ causes the magnetic induction $B(z)$ to penetrate over a depth $\lambda \equiv B(0)^{-1}\int B(z)dz$. In the London (*local*) limit, $B(z) \propto \exp(-z/\lambda_L)$, where λ_L is the London penetration depth. In 1953, to explain the variation of λ in Sn due to a change of the mean-free-path ℓ, Pippard proposed that the current density is related to the average of the vector potential over a region of size ξ_0 (the Pippard coherence length).[1] More recently the concept of nonlocality was applied to high-T_c cuprates.[2]

In the nonlocal theory $B(z)$ deviates from a simple exponential decay; it is *nonmonotonic* and, moreover, *changes sign* at a specific depth.[1] In the pure limit ($\xi_0 \ll \ell$) $B(z)$ is a function of the intrinsic parameters $\lambda_L(T=0)$ and ξ_0, and the temperature T. The magnitude of this *nonlocal* effect is determined by the ratio $\xi_0/\lambda_L(0) \propto 1/\kappa$; the smaller the Ginzburg-Landau parameter κ, the bigger the nonlocal effect. It is most significant in "extreme" type-I superconductors, such as Al ($\kappa \approx 0.01$) and In (0.06). For these the results of the Pippard theory are identical to those of the Bardeen-Cooper-Schrieffer theory,[3] in which nonlocality follows from the spatial separation of electrons in Cooper pairs. Thus, if confirmed, the nonlocal effect allows one to *measure* the size of the Cooper pairs (ξ_0) and $\lambda_L(0)$, which are currently calculated using the theory.[3]

$B(z)$ in In, calculated in local and nonlocal approaches, with $\xi_0=0.38$ μm and $\lambda_L(0)=0.025$ μm,[4] for $T=1.8$ K, is shown in Fig. 1. Details on the formalism can be found in Ref. 5. In the nonlocal approach $B(0)/e \approx B(2\lambda_L)$. The sign reversal is expected at $z \approx 5.5\lambda_L$, and the amplitude of the reversed field is about $0.03B(0)$. Indium is chosen due to its convenience for experiment.

An observation of sign reversal was reported in Ref. 6. An external ac magnetic field H with amplitude up to 30 Oe was applied parallel to a cylindrical Sn film, and a strongly attenuated (10^8 times) signal with reversed phase was detected inside the cylinder at 2.88 K and 25 Oe. It was interpreted as a sign change in the penetrating field. However, this interpretation is questionable because the phase difference drops back to zero at a larger (30 Oe) field, whereas the critical field H_c at 2.9 K is 115 Oe.[7]

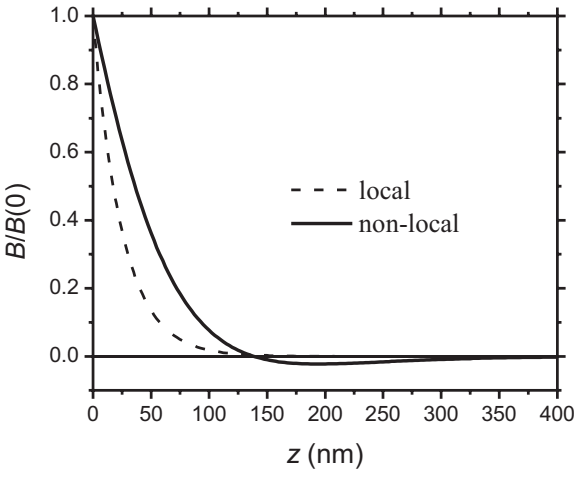

FIG. 1. Magnetic-induction profiles $B(z)$ in a semi-infinite In sample. The dashed (solid) line corresponds to the local (nonlocal) relation between current density and vector potential.

Nowadays $B(z)$ can be measured directly using PNR (Ref. 8) and low-energy muon spin rotation (LE-μSR) (Ref. 9) techniques. We comment briefly on the latter before focusing on the former.

In the LE-μSR technique polarized μ^+ (lifetime 2.2 μs) are implanted in a sample over a distance determined by the muon energy. $B(z)$ is obtained from the precession frequency of the muon spins at stopping distance. However, in practice the muon precession is strongly damped due to a broad distribution of stopping distances.[10] This is the main difficulty in applying the LE-μSR technique to fields with a sharp profile.

Recently the LE-μSR technique was used to measure $B(z)$ in Pb, Nb, and Ta.[10] Most interesting is the reported nonexponential shape of $B(z)$ for all these metals. The nonlinearity of $\log B(z)$ plots is marginal, which is coherent with the theory in view of the fairly high κ of the studied samples. For example, κ of pure Nb (residual resistivity ratio $RRR=1600$) is 1.3 at 3 K and 1.0 at 7 K.[11] However, in Ref. 10 κ of less pure Nb ($RRR=133$) is reported to be 0.7(2). This inconsistency with established literature data suggests that the muon probing results may contain some hidden uncertainties. Therefore, additional experiments would be worthwhile, in particular to verify the reliability of these results.

The PNR technique is based on the change of the neutron index of refraction in a magnetized medium. When a polarized neutron beam is incident on a laterally uniform sample under a grazing angle, its specular reflectivity R is determined by the profile of the neutron-scattering potential below the surface. R is measured versus momentum transfer $Q=4\pi \sin\theta/\lambda_n$, where θ is the angle of incidence and λ_n is the neutron wavelength. The scattering potential consists of a nuclear and a magnetic part, which results in different reflectivities R^+ and R^- for neutrons with spins parallel (up) and antiparallel (down) to the applied field, respectively. The sample magnetization is obtained from the spin asymmetry $s=(R^+-R^-)/(R^++R^-)$ by fitting $s(Q)$ data with $s(Q)$ simulations based on theoretical models for $B(z)$. The neutron reflectivity also depends on some other spin-independent parameters such as beam divergence $\delta\theta/\theta$; these parameters are determined independently and fine tuned using R-data for a nonmagnetized sample. Then $s(Q)$ is *solely* determined by the sample magnetization. PNR has been applied for measuring superconducting properties of Nb,[12,13] high-T_c cuprates[14–16] and Pb.[17,18]

The nonlocal effect in $B(z)$ measured with PNR was discussed in Refs. 12, 13, 17, and 18. Although some deviation from exponential decay was noticed in Refs. 13 and 17, no confirmation of the nonlocal theory was obtained. The authors of Ref. 18 correctly pointed out that experiments with lower-κ materials are desirable to verify nonlocality, but their overall conclusion was that PNR is incapable of detecting nonlocality in *any* superconductor.

Figure 2 shows $s(Q)$ calculated for an In layer with the "local" and "nonlocal" field profiles; details on the formalism are available in Ref. 19. The simulations indicate that the difference between spin asymmetries for the local and nonlocal approaches can be of the order of 10%, which is feasible for state-of-the-art PNR facilities. Therefore it is interesting to reassess the problem of nonlocality with PNR applied to a low-κ material.

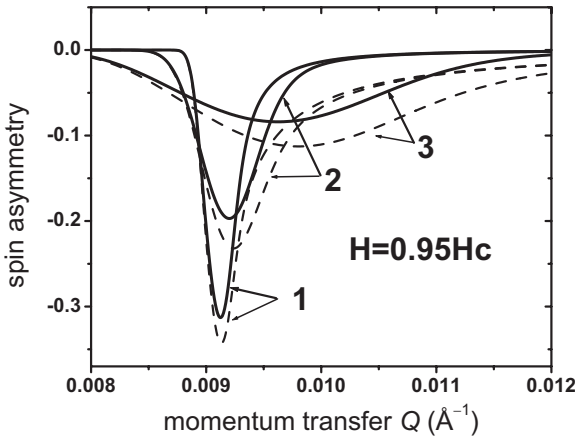

FIG. 2. Simulations of $s(Q)$ for a semi-infinite In layer based on the local (dashed lines) and on the nonlocal (solid lines) approaches. The instrumental resolution $\Delta Q/Q$ is 0.01, 0.03 and 0.1 for the curves 1, 2 and 3, respectively.

The design of the sample for the PNR study is based on the following requirements: The irradiated surface must be flat and possess minimal possible roughness. The sample must be thick enough to have the same properties as the bulk material. Degradation of the surface quality with increasing thickness limits the film thickness. Neutrons reflected back from the substrate should have a negligible effect on the reflectivity in a region close to the critical edge of total reflection, Q_c, where the reflectivity is most sensitive to the magnetic properties.

Two approaches can meet these requirements. One is to deposit a thick film on a flat substrate that reflects least. It can be achieved if the neutron refraction index of the substrate is larger than that of the sample. This approach was taken in the experiments on Nb (Refs. 12 and 13) and Pb.[17,18] In fact, this was the only option, in view of small absorption of neutrons in Nb and Pb. However, In is a strong absorber, which enables one to rely on substrates with a refractive index smaller than that of In, provided the film thickness d is properly optimized. In this approach a second plateau or "hill," associated with total reflection from the sample-substrate interface, is expected in the $R(Q)$ curve. This should yield additional information about the sample structure. Modeling shows that $d\approx 2.5$ μm is appropriate. Such a sample was fabricated in the present work.

High-purity indium (99.9999%) was deposited by thermal evaporation on the polished side of a silicon oxide wafer at room temperature. The substrate size was 2×2 cm^2 $\times 1$ mm. The base pressure and the evaporation rate were 4×10^{-8} mbar and 60–70 Å/s, respectively. The nominal film thickness, as recorded by a quartz monitor, was 2.5 μm. Several smaller area samples were simultaneously fabricated for the film characterization.

The root-mean-square (rms) surface roughness σ probed with an atomic force microscope (AFM) yielded 2.0, 6.7, and 8.0 nm at the scale of 1, 5, and 10 μm, respectively. A scan range up to 10 μm was not sufficient to reach saturation of the roughness. Consequently, 8.0 nm is a lower bound on σ at the scale of the neutron coherence length ($\approx$100 μm) (Ref. 20). Due to that, in simulations σ was allowed to vary to fit the experimental data.

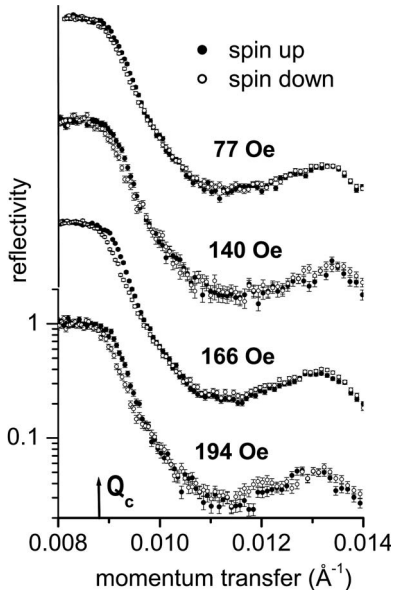

FIG. 3. Reflectivity of polarized neutrons in the Meissner state. Q_c is the momentum transfer for total neutron reflection from the outer surface. The scale is shown for the data at $H=194$ Oe; the other data have been shifted for clarity.

Another parameter associated with the sample surface is the thickness of the indium oxide film. When exposed to air, In, like its neighbors in the Periodic Table, Al and Ga, instantly forms a protective oxide layer. A surface of indium in air remains lustrous for years. This suggests that the oxide layer is very thin, perhaps of the order of a few monolayers, and should not affect the neutron reflectivity.[8] This is consistent with the negative result of Rutherford backscattering (RBS) measured on our sample: No oxide film has been detected.

The electromagnetic properties of the sample were characterized by the measured dc magnetization M and electrical resistivity. The shape of the $M(H)$ curves is typical for type-I superconductors. The obtained phase diagram $H_c(T)$ agrees well with the literature data.[7] T_c of our sample (3.415 K) matches the tabulated value of 3.4145 K,[21] and $RRR=540$. Correspondingly, $\ell \approx 11$ μm is much larger than ξ_0. Therefore, our sample is a type-I superconductor in the pure limit.

PNR experiments were performed on the REMUR reflectometer[22] at the Joint Institute for Nuclear Research (Dubna) and on the CRISP instrument[23] at ISIS (Oxford). Both sets of measurements confirm that splitting of the $R^+(Q)$ and $R^-(Q)$ curves is achievable for our sample. The ISIS data, which are the most detailed, allow a quantitative analysis to which we now turn.

CRISP operates with a spin-polarized polychromatic pulsed neutron beam. The angle θ and $\Delta Q/Q$ were set to 0.24 degrees and 3%, respectively.

The reflectivity in the Meissner state was measured at $T=1.8$ K and $H=77$, 140, 166, and 194 Oe [$H_c(1.8\ \text{K})=205$ Oe]. The obtained data sets are shown in Fig. 3. The $R(Q)$ dependencies exhibit a hill caused by total reflection from the substrate. The splitting between R^+ and R^- is clearly visible near Q_c; different magnitudes of the error bars are due to different times of exposure. The data obtained at 77 and 166 Oe have the smallest statistical error and will be used for further discussion.

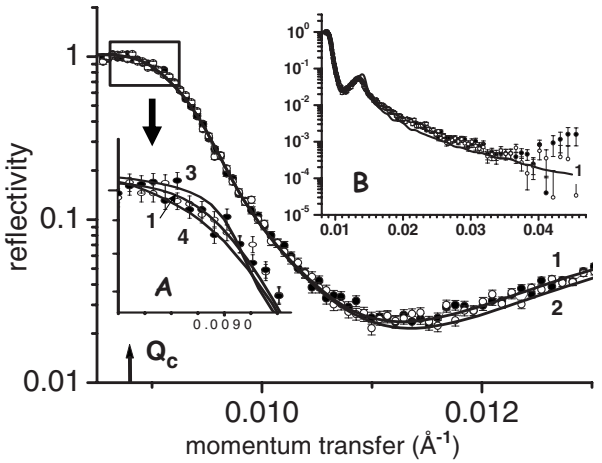

FIG. 4. Reflectivity data in the normal state. Curves 1 and 2 are simulations for $\Delta Q/Q=2.5\%$, $\sigma=14$ nm, and $d=2.40$ and 2.50 μm, respectively. Curves 3 and 4 in the inset A are simulations for $\Delta Q/Q=1\%$ and 4%, respectively. The inset B shows the data for the full range of Q values.

The data obtained in the normal state ($T=4.6$ K) are shown in Fig. 4. Solid curves are simulations, in which the sample is a pure In film on a SiO_2 substrate. In the simulations $\Delta Q/Q$ was allowed to vary due to the unknown uncertainties of the set value and of the geometrical factor (as only part of the beam covers the sample).

The simulation curve near Q_c is mostly controlled by the resolution (see Fig. 4 and, e.g., Ref. 17). The next segment, down to the foothill, is determined by the roughness of the sample surface. The location of the ascending part [$0.011 < Q(\text{Å}^{-1}) < 0.014$] is governed by the film thickness. The segment following the hill is determined by the substrate scattering properties. No attempts were made to achieve a better fit for that segment, because there the spin asymmetry is indistinguishable from zero.

The best fit (curve 1 in Fig. 4) was obtained for the model sample with $\sigma=14$ nm and $\Delta Q/Q=2.5\%$. Fitting the ascending part enables one to determine d *in situ*. The statistical error of the reflectivity data in this region being $\pm 5\%$, the thickness was found to be 2400 ± 30 nm, in agreement with the nominal thickness of 2.5 μm. These parameters were further used for simulating the spin asymmetry. Attempts to introduce an indium oxide layer on top of the sample yielded no reasonable fit for any appreciable thickness (>1 nm) of the oxide layer. This is consistent with our expectation that the indium oxide layer does not affect the neutron reflectivity.

Simulations of the reflectivity in the Meissner state were performed assuming on both sides of the sample the field profiles shown in Fig. 1. The $s(Q)$ data for fields 77 Oe and 166 Oe, along with simulations for the local and nonlocal field distributions, are shown in Fig. 5.

For field 77 Oe [Fig. 5(a)], the results of the "nonlocal" simulation fit the experimental data somewhat better, but no clear discrimination between the local and nonlocal approaches is possible due to insufficient accuracy of these

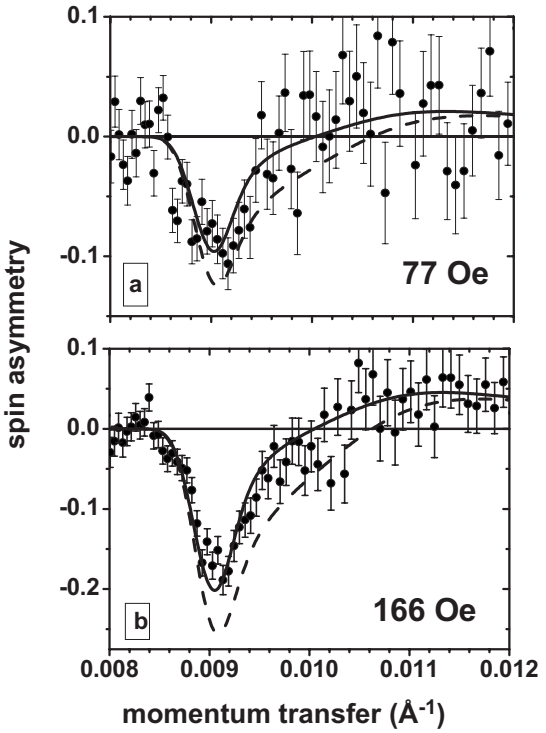

FIG. 5. Spin asymmetry at $T=1.8$ K and $H=77$ Oe (a) and 166 Oe (b). The curves are simulations performed within the local (dashed line) and nonlocal (solid line) approaches.

data. A significantly clearer distinction is apparent for field 166 Oe due to the larger amplitude of $s(Q)$. As can be seen from Fig. 5(b), the quality of the fits, with $B(z)$ calculated in the local and nonlocal approaches, is different. The nonlocal curve fits the experimental data definitely better. It is worth stressing that *no adjustable parameters* have been used for calculations of the spin asymmetry.

In conclusion, nonlocal electrodynamics effects are measurable, at least in extreme type-I superconductors. State-of-the-art PNR measurements performed on In unambiguously support the nonlocal theory and at the same time demonstrate consistency with the literature data for $\lambda_L(0)$ and ξ_0. Consequently, evidence has been gathered for the nonmonotonic decay and sign reversal of the penetrating magnetic field predicted by the nonlocal electrodynamics approach.

We thank A. Volodin for AFM, S. Vandezande for resistivity, and A. P. Kobzev for RBS measurements. This research was supported by the KULeuven Research Council (Grants No. F/05/049 and GOA/2004/02), Projects No. G.0237.05, G.0115.06, and G.0356.06 of FWO-Vlaanderen, IUAP P5/1, the European Commission under the 6th Framework Programme through the Key Action: Strengthening the European Research Area, Research Infrastructures (Contract No. HII3-CT-2003-505925), Russian State (Contract No. 2007-3-1.3-07-01), INTAS (Grant No. 03-51-6426), and RFBR (Project No. 06-02-16221).

*Present address: Interdisciplinary Research Institute, CNRS USR 3078, 59021 Lille, France.

[1] A. B. Pippard, Proc. R. Soc. London, Ser. A **216**, 547 (1953).
[2] I. Kosztin and A. J. Leggett, Phys. Rev. Lett. **79**, 135 (1997).
[3] M. Tinkham, *Introduction to Superconductivity* (McGraw-Hill, New York, 1996).
[4] P. Valko, M. R. Gomes, and T. A. Girard, Phys. Rev. B **75**, 140504(R) (2007); K. S. Wood and D. Van Vechten, Nucl. Instrum. Methods Phys. Res. A **314**, 86 (1992).
[5] J. Halbritter, Z. Phys. **243**, 201 (1971).
[6] K. E. Drangeid and R. Sommerhalder, Phys. Rev. Lett. **8**, 467 (1962).
[7] D. K. Finnemore and D. E. Mapother, Phys. Rev. **140**, A507 (1965).
[8] G. P. Felcher, Physica B (Amsterdam) **192**, 137 (1993).
[9] E. Morenzoni, F. Kottmann, D. Maden, B. Matthias, M. Meyberg, Th. Prokscha, Th. Wutzke, and U. Zimmermann, Phys. Rev. Lett. **72**, 2793 (1994).
[10] A. Suter, E. Morenzoni, N. Garifianov, R. Khasanov, E. Kirk, H. Luetkens, T. Prokscha, and M. Horisberger, Phys. Rev. B **72**, 024506 (2005).
[11] D. K. Finnemore, T. F. Stromberg, and C. A. Swenson, Phys. Rev. **149**, 231 (1966).
[12] G. P. Felcher, R. T. Kampwirth, K. E. Gray, and R. Felici, Phys. Rev. Lett. **52**, 1539 (1984).
[13] H. Zhang, J. W. Lynn, C. F. Majkrzak, S. K. Satija, J. H. Kang, and X. D. Wu, Phys. Rev. B **52**, 10395 (1995).
[14] R. Felici, J. Penfold, R. C. Ward, E. Olsi, and C. Matacotta, Nature (London) **329**, 523 (1987).
[15] A. Mansour, R. O. Hilleke, G. P. Felcher, R. B. Laibowitz, P. Chaudhari, and S. S. P. Parkin, Physica B (Amsterdam) **156-157**, 867 (1989).
[16] V. Lauter-Pasyuk, H. J. Lauter, V. L. Aksenov, E. I. Kornilov, A. V. Petrenko, and P. Leiderer, Physica B (Amsterdam) **248**, 166 (1998).
[17] K. E. Gray, G. P. Felcher, R. T. Kampwirth, and R. Hilleke, Phys. Rev. B **42**, 3971 (1990).
[18] M. P. Nutley, A. T. Boothroyd, C. R. Staddon, D. McK. Paul, and J. Penfold, Phys. Rev. B **49**, 15789 (1994).
[19] S. J. Blundell and J. A. C. Bland, Phys. Rev. B **46**, 3391 (1992).
[20] K. Temst, M. J. Van Bael, and H. Fritzsche, Appl. Phys. Lett. **79**, 991 (2001).
[21] *Handbook of Physical Quantities*, edited by I. S. Grigoriev and E. Z. Meilikhov (CRC, New York, 1997).
[22] V. L. Aksenov, K. N. Jernenkov, S. V. Kozhevnikov, H. Lauter, V. Lauter-Pasyuk, Yu. V. Nikitenko, and A. V. Petrenko (www.jinr.ru/publish/Preprints/2004/047(D13-2004-47)e.pdf).
[23] D. G. Bucknall, S. Langridge, and R. M. Dalgliesh (www.isis.rl.ac.uk/largescale/crisp/).